J. Membrane Biol. 23, 305–347 (1975)

A Model of NaCl and Water Flow Through Paracellular Pathways of Renal Proximal Tubules

Ronald E. Huss and Donald J. Marsh

Biomedical Engineering, Graduate Center for Engineering Sciences, University of Southern California, Los Angeles, California 90007

Received 24 March 1975; revised 27 May 1975

Summary. To explain how hydrostatic pressure differences between tubule lumen and interstitium modulate isotonic reabsorption rates, we developed a model of NaCl and water flow through paracellular pathways of the proximal tubule. Structural elements of the model are a tight junction membrane, an intercellular channel whose walls transport NaCl actively at a constant rate, and a basement membrane. Equations of change were derived for the channel, boundary conditions were formulated from irreversible thermodynamics, and a pressure-area relationship typical of thin-walled tubing was assumed. The boundary value problem was solved numerically. The principal conclusions are: 1) channel NaCl concentration must remain within a few mOsm of isotonic values for reabsorption rates to be modulated by transtubular pressure differences known to affect this system; 2) basement membrane and channel wall parameters determine reabsorbate tonicity; tight juction parameters affect the sensitivity of reabsorption to transmural pressure; 3) channel NaCl concentration varies inversely with transmural pressure difference; this concentration variation controls NaCl diffusion through the tight junction; 4) modulation of NaCl diffusion through the tight junction controls the rate of isotonic reabsorption; modulation of water flow can increase sensitivity to transmural pressure; 5) no pressure-induced change in permeability of the tight junction or basement membrane is needed for pressure to modulate reabsorption; and 6) system performance is indifferent to the distribution of active transport sites, to the numerical value of the compliance function, and to the relationship between lumen and cell pressures.

Glossary of Symbols

A	channel cross-section area, cm^2
A_{max}	maximum channel cross-section area, cm^2
α	volume flow rate, dimensionless
b	NaCl concentration gradient, $(mOsm\ cm^{-4}) \times 10^{-3}$
β	NaCl concentration gradient, dimensionless
C	NaCl concentration, $(mOsm\ cm^{-3}) \times 10^{-3}$
$\bar{C}$	arithmetic mean NaCl concentration $(mOsm\ cm^{-3}) \times 10^{-3}$
γ	NaCl concentration, dimensionless
D	channel NaCl diffusion coefficient, $cm^2\ sec^{-1}$
E	emergent osmolality, $(mOsm\ cm^{-3}) \times 10^{-3}$

k_1 channel wall hydraulic permeability, dimensionless
k_2 NaCl active transport rate, dimensionless
k_3 basement membrane hydraulic permeability, dimensionless
k_4 tight junction hydraulic permeability, dimensionless
k_5 basement membrane NaCl permeability, dimensionless
k_6 tight junction NaCl permeability, dimensionless
k_7 NaCl reflection coefficient, tight junction, dimensionless
k_8 NaCl reflection coefficient, basement membrane, dimensionless
L hydraulic permeability, cm sec^{-1} mm Hg^{-1} or NaCl permeability, cm sec^{-1}
λ distance, dimensionless
N NaCl active transport rate, mOsm cm^{-2} sec^{-1}
ξ compliance parameter, mm Hg^{-1}
p hydrostatic pressure, mm Hg
$\bar{p}$ cell hydrostatic pressure, mm Hg
Π osmotic pressure, mm Hg
q volume flow rate, cm^3 sec^{-1}
R universal gas constant, mm Hg T^{-1} mol^{-1}
r A/A_{max}, dimensionless
S channel circumference, cm
σ NaCl reflection coefficient
T absolute temperature, °K
Φ hydrostatic pressure, dimensionless
X channel length, cm
x distance, cm
z pump distribution, dimensionless

Subscripts

B basement membrane
BS basement membrane, NaCl
IS interstitial space
L lumen
o isotonic
T tight junction
TS tight junction, NaCl

Isotonic fluid reabsorption by the renal proximal tubule is powered by active transport of NaCl, but the rate of fluid reabsorption is known to vary with the levels of hydrostatic and colloid osmotic pressure in the plasma of blood perfusing peritubular capillaries [4, 5, 6, 8, 12, 24, 27, 29]. When changes in these pressures increase the movement of fluid from interstitial space to capillary lumen, the rate of fluid reabsorption by the tubule increases; pressure changes in the opposite direction inhibit tubular fluid reabsorption. Because this modulation of reabsorptive rate involves no obvious chemical signalling, there is considerable interest in providing a mechanism that does not require selective control of the

rate of active transport. Attention has therefore focussed on whether the passive elements of the system are responsible for the modulation of reabsorption.

A change in the rate of fluid removal by the capillaries will change interstitial hydrostatic pressure, and with it, the transtubular hydrostatic pressure difference. The region of the tubule wall most likely to respond to changes of transtubular hydrostatic pressure is the complex formed by the tight junction and the lateral intercellular channel. The intercellular channel was first suggested as the route of fluid reabsorption in the gallbladder [18, 32]. Tormey and Diamond [32] concluded that the narrow confines of these channels provide a restricted space in which osmotic equilibration could proceed to isotonicity before the reabsorbed fluid entered the interstitial space. Diamond and Bossert [10] showed by means of a mathematical model that this pathway was capable, at least in principle, of generating an isotonic absorbate. But hydrostatic pressure is not a variable in Diamond and Bossert's model, so that modulation of reabsorptive rate by hydrostatic pressure cannot be predicted unless the model is modified.

More recent studies [3, 9, 12–15, 17, 27, 32] have brought to light the fact that the tight junction provides a relatively low resistance shunt pathway for the movement of ions between the lumen and the intercellular channel. The question has naturally arisen whether the flow of NaCl, of water, or of both, across the tight junction might be responsive to the transtubular hydrostatic pressure difference. The results of several studies imply rather strongly that reduction of the transtubular hydrostatic pressure difference leads to dilatation of the intercellular channels [3, 11, 17, 27, 30]. Although it is easy to understand how this pressure difference might affect the extent of dilatation of the channels, it is less clear how flow processes at the tight junction might be influenced.

We have formulated a mathematical model of the tight junction-lateral intercellular channel complex. Our broad goal is to achieve some qualitative understanding of the interactions between tight junction transport processes and the formation of an isotonic reabsorbate, and the dependence of these processes on the transmural hydrostatic pressure. We undertook this effort despite the lack of sufficient data to yield a unique solution, and despite the lack of techniques for measuring NaCl concentration or volume flow rate in the small confines of the channel that could test the model, because the boundary value problem is so nonlinear that it defies intuitive understanding. The results suggest some constraints on

the operation of the system that have not emerged from the simpler model of Diamond and Bossert [10].

Derivation of Equations

The derivation of the differential equations follows the lines used by Diamond and Bossert [10], except that we introduce the channel pressure as a new dependent variable (or free parameter) of the system. We consider the channel to be a cylinder of length X, having a constant circumference S, and having a uniform cross-sectional area A over its length, as shown in Fig. 1. The channel is assumed to be compliant with a maximum area A_{max}. Located along the walls are pumps which move solute from the cell interior into the channel. The walls are otherwise impermeable to solute.

Some measurements suggest that the Na^+ and Cl^- permeabilities of the peritubular membrane are small but not zero [36]; by extension, the

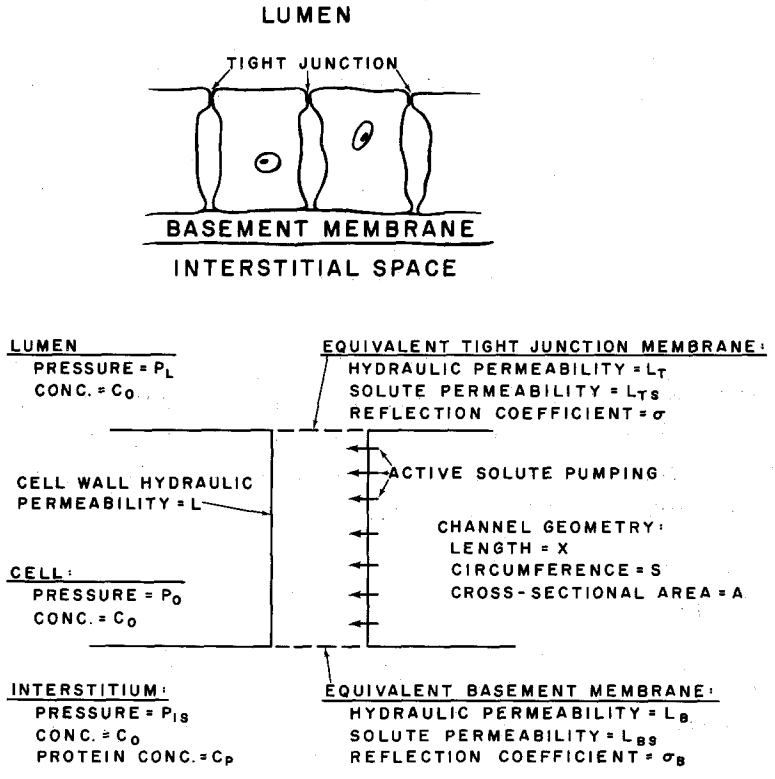

Fig. 1. Diagram of a section of proximal tubule wall, and the idealized channel as it is used in the model

channel walls might also be permeable. The experiments on which these conclusions are based were designed under the assumption that all ionic fluxes crossed the epithelial cells. But the paracellular pathway was also available to the tracers used, and so the values of peritubular membrane permeability are probably overestimates. For the purposes of this model, we simply assume that passive NaCl flow through the channel wall is negligibly small in comparison to other processes contributing to mass balance, but not necessarily zero.

Consider a short segment of the channel between x and $x+\Delta x$; if $q(x)$ is the volume flow rate at x, then the difference between $q(x+\Delta x)$ and $q(x)$ is the rate of fluid flow through the wall. This flow is proportional to the wall area ($S\Delta x$), the unit hydraulic permeability (L), and the total transmural hydrostatic and osmotic pressure difference across the channel wall. The channel hydrostatic pressure is p, and the cell pressure is $\bar{p}$; the osmotic pressure of the channel fluid is $\Pi(x)$. We assume the cell interior to be isotonic, therefore we denote its osmotic pressure as Π_o. Standard analytic techniques yield the differential equation

$$\frac{dq}{dx} = SL[(\bar{p}-p)+(\Pi(x)-\Pi_o)], \qquad 0 \leqq x \leqq X. \tag{1}$$

The osmotic pressure is given by

$$\Pi(x) = RT\,C(x), \tag{2}$$

where $C(x)$ is the osmolar concentration of solute in the channel at x.

Solute moves into the channel segment between x and $x+\Delta x$ axially by diffusion and convection, and radially by active transport. The differential equation describing this process is second order; for convenience, we write it as two first-order equations,

$$\frac{dC}{dx} = b(x) \tag{3}$$

$$\frac{db}{dx} = \frac{1}{AD}\,q(x)\,b(x) + \frac{SLC(x)}{AD}[(\bar{p}-p)+(\Pi(x)-\Pi_o)] - \frac{S}{AD}N(x). \tag{4}$$

Here A is the channel cross-sectional area, D is the diffusion coefficient of NaCl, and $N(x)$ is the active pumping rate at x. The cross-sectional

area A we express as a fraction of the maximum cross-sectional area,

$$A = r A_{max}, \tag{5}$$

where $0 \leqq r \leqq 1$.

We assume that the ends of the channel are covered by uniform membranes. The boundary conditions are formulated using the equations of irreversible thermodynamics derived by Kedem and Katchalsky for homogeneous membranes [19]. We assume that each end process can be treated as a homogeneous membrane having a permeability equivalent to that of the actual end membrane. One important consideration in deriving the boundary conditions is the behavior of the end membrane geometry as the channel area changes. Micrographic data yield little insight, so we tested two conditions at each end. First, we assumed that the area of the actual end opening remains constant for all channel areas; second, we assumed that the end opening area remain a constant fraction of the channel area. These two views would appear to encompass all other relationships between membrane and channel area. We incorporate these conditions through a modification of the equivalent membrane permeabilities by the area ratio r.

For the tight junction, with constant area, the equation for fluid flow is

$$q(0) = L_T[(p_L - p) + \sigma(\Pi(0) - \Pi_L)], \tag{6}$$

while if the area varies in proportion to the channel area, the equation is

$$q(0) = L_T r[(p_L - p) + \sigma(\Pi(0) - \Pi_L)]. \tag{7}$$

In these equations, p_L and p are the hydrostatic pressures in the lumen and channel, respectively, and Π_L and $\Pi(0)$ the osmotic pressures on the luminal and channel sides, respectively, of the equivalent tight junction membrane. The reflection coefficient for NaCl is denoted by σ. The hydraulic permeability L_T is the area-adjusted permeability of the membrane with units $cm^3\ sec^{-1}\ mm\ Hg^{-1}$.

For solute flow across the tight junction when the area is constant, the conservation equation is

$$q(0)\ C(0) - AD\ b(0) = q(0)\ \bar{C}_T(1-\sigma) + L_{TS}[C_L - C(0)]; \tag{8}$$

if the area is proportional to the channel area, the relation becomes

$$q(0)\ C(0) - AD\ b(0) = q(0)\ \bar{C}_T(1-\sigma) + L_{TS} r[C_L - C(0)]. \tag{9}$$

Here $\bar{C}_T$ is an average concentration in the tight junction channel. Since the concentrations on both sides of the membrane are very close, we use the arithmetic mean of these two concentrations. As with the hydraulic permeability, the solute permeability L_{TS} is the area-adjusted permeability with units $cm^3\ sec^{-1}$.

At the basement membrane, we form similar conditions. For mass flow, when the area is constant, we write

$$q(X)=L_B[(p-p_{IS})+\sigma_B(\Pi_{IS}-\Pi(X))], \tag{10}$$

and when the area is variable,

$$q(X)=L_B r[(p-p_{IS})=\sigma_B(\Pi_{IS}-\Pi(X))]. \tag{11}$$

The terms p_{IS} and Π_{IS} are the hydrostatic and osmotic pressures, respectively, in the interstitial space. The NaCl reflection coefficient of the basement membrane is σ_B.

For solute flow across the basement membrane with constant area, we write

$$q(X)\ C(X)-AD\ b(X)=q(X)\ \bar{C}_B(1-\sigma_B)+L_{BS}[C(X)-C_{IS}]. \tag{12}$$

For variable area, the relation is

$$q(X)\ C(X)-AD\ b(X)=q(X)\ \bar{C}_B(1-\sigma_b)+L_{BS}r[C(X)-C_{IS}]. \tag{13}$$

Here, as in the equation for tight junction solute flow, we use the arithmetic mean of the concentrations on both sides of the membrane to approximate $\bar{C}_B$. For the first studies in this paper, we shall assume that both the tight junction and the basement membrane area are constant. In a later section, we shall show how the results are affected by our choice of the membrane geometries.

The formulation we have used assumes that NaCl moves as a single solute, rather than as dissociated Na^+ and Cl^- ions. When the only solute is a uniunivalent salt, the summation of the forces acting on the ion pair leads to cancellation of the electrical terms, because the valences are of equal magnitude but opposite sign. This summation is required to satisfy macroscopic charge neutrality. When the presence of other ions is taken into account, the formulation of the boundary conditions and of Eqs. (3) and (4) will have to include electrical terms.

Eqs. (1), (3) and (4) are the differential equations of the model, and the boundary conditions are given by Eqs. (6), (8), (10) and (12). Since there are only three equations, but four boundary conditions, we require one additional degree of freedom. We obtain this by allowing the channel pressure p to be a free parameter.

In all cases, we assume that the NaCl osmolar concentrations of the lumen, cell interior, and interstitium are isotonic (300 milliosmolar). Thus, C_L and C_{IS} are each replaced by C_o.

In order to simplify the study, we introduce certain dimensionless variables. Define a new distance variable λ as

$$\lambda = x/X. \tag{14}$$

Next, define a dimensionless flow variable as

$$\alpha(\lambda) = \frac{q(\lambda)}{\Pi_o SLX}. \tag{15}$$

The new dimensionless concentration variable is

$$\gamma(\lambda) = \frac{C(\lambda) - C_o}{C_o}; \tag{16}$$

$\gamma(\lambda)$ is an excess concentration over isotonicity. Finally, define a dimensionless concentration gradient as

$$\beta(\lambda) = \frac{X}{C_o} b(\lambda). \tag{17}$$

The hydrostatic pressures are normalized by dividing by Π_o. Thus, the channel pressure becomes

$$\Phi = \frac{p}{\Pi_o}, \tag{18}$$

the interstitial pressure becomes

$$\Phi_{IS} = p_{IS}/\Pi_o, \tag{19}$$

the lumen pressure is

$$\Phi_L = p_L/\Pi_o, \tag{20}$$

the cell pressure is

$$\bar{\Phi} = \bar{p}/\Pi_o. \tag{21}$$

We also introduce a number of dimensionless constants, defined as

$$k_1 = \Pi_o(SLX) \Big/ \left(\frac{A_{\max} D}{X}\right), \tag{22}$$

$$k_2 = \left(\frac{N_o}{C_o}\right) \Big/ \left(\frac{A_{\max} D}{X}\right), \tag{23}$$

$$k_3 = L_B/(SLX), \tag{24}$$

$$k_4 = L_T/(SLX), \tag{25}$$

$$k_5 = L_{BS} \Big/ \left(\frac{A_{\max} D}{X}\right), \tag{26}$$

$$k_6 = L_{TS} \Big/ \left(\frac{A_{\max} D}{X}\right), \tag{27}$$

$$k_7 = \sigma, \tag{28}$$

$$k_8 = \sigma_B, \tag{29}$$

$$r = A/A_{\max}. \tag{30}$$

All of the physical parameters in Eqs. (22)–(30) have been defined except for N_0. In Eq. (23), N_0 is the total rate of solute pumping into the channel, measured in milliosmoles per second. For the results to be described, we used a uniform pump distribution over the length of the channel. In a later section, we shall discuss the effects on the solution of other distributions.

Segel [28], who worked with the Diamond-Bossert model [10], showed that there exist a number of equally valid normalization procedures that can be used to convert equations of change for intercellular channels to dimensionless form. Our normalization procedure differs from Segel's in four respects. First, Segel scaled the length variable to the fraction of the channel length over which the pumps were localized; we used the length of the entire channel because we were primarily interested in simulating transport over the whole length of the channel. Second, Segel scaled the concentration variable to isotonic concentration; we scaled a concentration difference variable to isotonicity, because of the small

differences our preliminary simulations led us to anticipate. Third, we scaled hydrostatic pressures to the osmotic pressure of isotonic fluids; Segel did not consider the effects of pressure. Fourth, we scaled end membrane permeabilities to channel solute conductance or channel wall fluid conductance; Segel did not consider end membrane processes.

In terms of these dimensionless variables and parameters, the system equations are

$$\frac{d\alpha}{d\lambda}=\gamma(\lambda)+(\bar{\Phi}-\Phi), \tag{31}$$

$$\frac{d\gamma}{d\lambda}=\beta(\lambda), \tag{32}$$

$$\frac{d\beta}{d\lambda}=\frac{k_1}{r}\{\alpha(\lambda)\,\beta(\lambda)+[1+\gamma(\lambda)]\,[\gamma(\lambda)+(\bar{\Phi}-\Phi)]\}-\frac{k_2}{r}z(\lambda), \tag{33}$$

where

$$z(\lambda)=1, \quad 0\leqq\lambda\leqq 1, \tag{34}$$

with boundary conditions

$$\alpha(0)=k_4[\Phi_L-\Phi+k_7\gamma(0)], \tag{35}$$

$$\frac{k_1}{r}\alpha(0)\left[k_7+(1+k_7)\frac{\gamma(0)}{2}\right]-\beta(0)=-\frac{k_6}{r}\gamma(0), \tag{36}$$

$$\alpha(1)=k_3[\Phi-\Phi_{IS}-k_8\gamma(1)], \tag{37}$$

$$\frac{k_1}{r}\alpha(1)\left[k_8+(1+k_8)\frac{\gamma(1)}{2}\right]-\beta(1)=\frac{k_5}{r}\gamma(1). \tag{38}$$

(In Eq. (36), $z(\lambda)$ is the pump distribution function normalized to $N_0=1$.)

One other quantity of interest is the osmolality of the emergent fluid. This is the ratio of the rate of solute flow to the rate of fluid flow across the basement membrane. The solute flow is given by the right-hand side of Eq. (12), and the water flow is $q(x)$. Letting E represent the emergent osmolality, we write

$$E=\frac{q(X)\left[\dfrac{C(X)+C_o}{2}\right](1-\sigma_B)+L_{BS}[C(X)-C_{IS}]}{q(X)}. \tag{39}$$

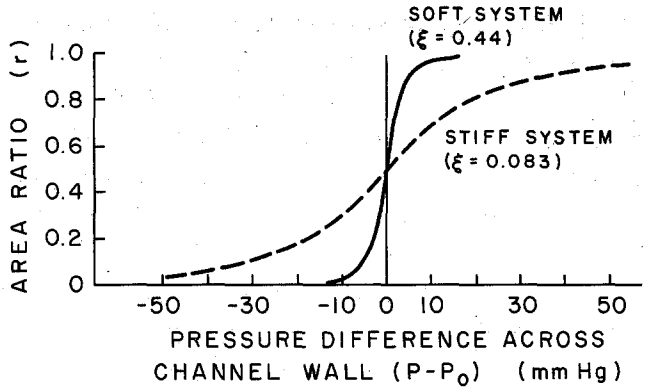

Fig. 2. Channel compliance curves as used in the model, showing a soft function and a stiff function

Substituting for $q(X)$ and $C(X)$ from Eqs. (10), (15) and (16), and using the expressions for the dimensionless parameters k_3 and k_5 from Eqs. (24) and (26), this reduces to

$$E = C_o \left[\left(1 + \frac{\gamma(1)}{2} \right) (1 - k_8) + \frac{k_5 \gamma(1)}{k_1 k_3 (\Phi - \Phi_{IS} - k_8 \gamma(1))} \right]. \tag{40}$$

In order to determine how the flow responds to pressure changes across the epithelium, we require a relation between channel pressure and channel cross-section area. We consider the channels to be thin-walled tubes. As such, the compliance function would be expected to have a characteristic sigmoidal shape, which can be approximated by a hyperbolic tangent function. If we let r be the ratio of channel area to the maximum channel area, then typical compliance curves, as shown in Fig. 2, have the equation

$$r = \frac{1}{1 + e^{-\xi(p - \bar{p})}}, \tag{41}$$

where $(p - \bar{p})$ is the pressure difference between channel and cell, and ξ is a constant. The value of this constant determines the stiffness of the system. If ξ is large, then the system is very soft, that is, the area changes rapidly in response to small pressure changes, then the channel pressure is near the cell pressure. For our basic parameter set, we chose a fairly stiff function, where ξ was 0.083. With this value, a pressure difference of 26.5 mm Hg is required to change the cross-sectional area

from 0.5 to 0.9 of the maximum. Further discussion of the sensitivity of the system to our choice of ξ will be given in a later section.

Numerical Results

The boundary value problem of Eqs. (31)–(38) was solved numerically via quasilinearization [2]. The integration was carried out using a fourth order Adams-Moulton predictor-corrector method with a step size of 0.01 in λ. All calculations were performed by an IBM 370/158 digital computer. Convergence was obtained when a solution was within 0.1 percent of the solution from the previous iteration.

Our first estimates of the values of the dimensionless parameters were made by estimating minimum and maximum values of the physical parameters that comprise them. The extrema of $k_1, k_2, \ldots, k_6$ generally differed by 8 to 10 orders of magnitude. Preliminary numerical experiments quickly showed that for the model to yield physiologically reasonable results, the values of the dimensionless parameters would have to be confined to considerably narrower ranges. We shall discuss each of the parameters in detail.

k_1: This parameter is the ratio of the water permeability of the channel wall (SLX) to the axial diffusion permeability of the channel ($A_{\max} D/X$). The larger this ratio is, the greater is the flux of water across the wall; this leads to more rapid osmotic equilibration of the channel fluid.

The minimum value of k_1 occurs when (SLX) is minimum and ($A_{\max} D/X$) is a maximum. The channel length X we estimated from micrographs [25] to lie between 30 and 100 μ. For the circumference S we note that Diamond and Bossert have estimated the widths of channels in transporting epithelia, and quote values from 0.01 to 1 μ [10]. If we assume that these values are for near maximally distended channels having approximately circular cross-sections, the circumference ranges from 0.05 to 5 μ. From these same estimates of channel width, we find that the value of $A_{\max}$ lies between 10^{-12} and 10^{-8} cm^2.

The diffusion coefficient D for NaCl in free solution at low concentrations is 1.47×10^{-5} cm^2/sec [26]. However, in these restricted channels, the value may be somewhat lower. For example, Spring [30] assumes that the value may be only 1/5 of its free solution value. We would expect D, then, to lie between 0.3×10^{-5} and 1.47×10^{-5} cm^2/sec.

Numerical values of the wall permeability L are the least reliable of the parameter values. A possible guide is the overall hydraulic permeability

of the epithelium. Ullrich [33] cites experimental measurements of rat proximal tubule permeability in the range 1.5×10^{-7} to 7.3×10^{-8} cm sec^{-1} mm Hg^{-1}. Since a part of the flow measured in those studies may have been through the tight junction-intercellular channel and not through the cell, these values would overestimate the cell membrane permeability. We thus estimate that the value of L will lie between 10^{-10} and 10^{-7} cm sec^{-1} mm Hg^{-1}.

Using these values, we find that the range of SLX is from 1.5×10^{-18} to 5×10^{-13} cm^3 sec^{-1} mm Hg^{-1}, and the range of $A_{max}D/X$ is from 3×10^{-16} to 5×10^{-11} cm^3 sec^{-1}. Using these extrema, the range of k_1 is from 2×10^{-4} to 1×10^{7}.

k_2: The parameter k_2 is the ratio of the rate at which solute is pumped into the channel to the rate of axial diffusion. One estimate of the range of values of N_0 is given in Ref. [14] as 10^{-9} to 10^{-14} osmoles per sec per cm^2 of channel wall area. The channel wall area SX lies between 1.5×10^{-8} cm^2 and 5×10^{-6} cm^2, so the value of N_0 will lie between 10^{-14} and 10^{-22} osmoles/sec. Since mammalian proximal tubule shows a high transport rate, we shall confine our studies to the higher values, and even extend the range, so N_0 will be in the range 10^{-16} to 10^{-13} osmoles/sec.

Using this range for N_0 and the range of $(A_{max}D/X)$ determined above, we find that the value of k_2 will lie between 10^{-2} and 10^{6}.

k_3, k_4: These are the ratios of the equivalent end membrane hydraulic permeabilities to the total channel wall hydraulic permeability. Although the hydraulic permeability of the basement membrane has been determined in one experiment [35], the geometry of the basement membrane process is sufficiently indeterminate so that we were unable to assert a definite value for the total membrane permeability. At the tight junction, even less is known of the properties. Because of these uncertainties, we chose to look at the system behavior when the hydraulic permeabilities were substantially larger or substantially smaller than the side wall permeabilities. Accordingly, we allowed k_3 and k_4 to take values between 10.0 and 0.01.

k_5, k_6: These are the ratios of the solute permeabilities of the basement membrane and the tight junction membrane, respectively, to the axial diffusion permeability of the channel, $A_{max}D/X$. As with the hydraulic permeabilities, reliable data are lacking, so we allowed these parameters to assume values between 10.0 and 0.01.

k_7, k_8: These dimensionless constants are the osmotic reflection coefficients of the tight junction channel and the basement membrane, respec-

tively. We assumed a value of 0.3 for k_7, and for k_8 we assumed 0.01. We shall show later how the values of these parameters affect the system behavior.

In order to choose a representative set of values, we varied the parameters within the ranges given above until the solution satisfied two criteria:

1. The reabsorbate must be essentially isotonic, which we have defined as being within 2% of exact isotonicity.
2. The reabsorptive flow must be responsive to changes in the transepithelial pressure difference; Spitzer and Windhager [29] show that where the peritubular oncotic pressure is increased from 0 to 30 mm Hg, the reabsorptive flow increases by approximately 25 percent. If we assume that interstitial pressure varies directly with capillary pressure, then we set this response as a goal for the model.

Preliminary numerical studies led us to select the following set of dimensionless parameters, which satisfy the criteria reasonably well: $k_1=12.0$, $k_2=0.03$, $k_3=1.0$, $k_4=0.1$, $k_5=0.05$, $k_6=1.0$, $k_7=0.3$, $k_8=0.005$. The results discussed in the following paragraphs were obtained using this reference parameter set. The value of N_0, the total solute pumping rate, was taken to be 10^{-15} osmoles/sec. In all the simulations we carried out, lumen pressure was held constant at 10 mm Hg, and interstitial pressure was allowed to vary from 10 to -30 mm Hg. The convention used to define the pressure difference was lumen pressure minus interstitial pressure. A pressure difference of 0 mm Hg means that both lumen and interstitial pressures are 10 mm Hg; a pressure difference of 20 mm Hg means that lumen pressure is 10 mm Hg and interstitial pressure is -10 mm Hg. Except in one set of simulations where cell hydrostatic pressure was deliberately varied, the cell pressure was assumed to be the same as lumen pressure, or 10 mm Hg. The reason for assuming cell and lumen pressure to be the same is the finding that the basement membrane by itself accounts for virtually all of the elastic properties of the isolated perfused proximal tubule [35].

Figs. 3 and 4 show the channel concentration and volume flow rate profiles at transmural hydrostatic pressure differences of 0 and 20 mm Hg. In both cases, the NaCl concentration is nearly constant along the length of the channel. Since the rate of active transport is the same in both cases, the concentration is a function primarily of the volume flow rate; the higher the flow rate, the lower the concentration. The channel concentration is less than isotonic at 20 mm Hg transmural pressure difference

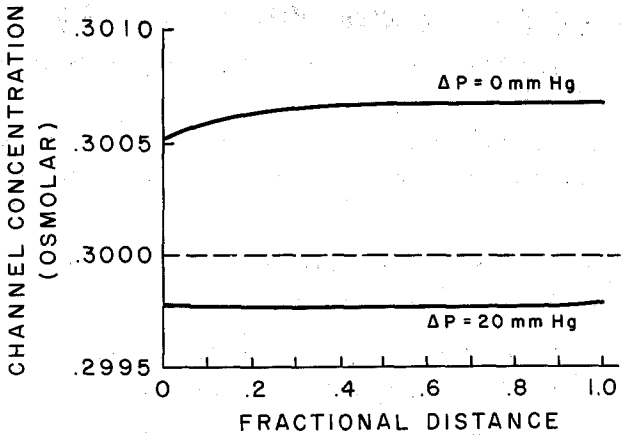

Fig. 3. Channel concentration profiles for two transmural pressure differences. The parameter set is the reference set as given in the text

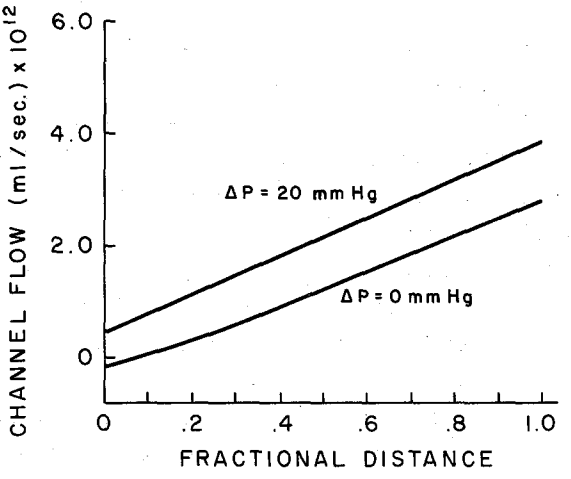

Fig. 4. Channel flow profiles for two transmural pressure differences. The parameter set is the reference set given in the text

(and also at larger pressure differences) because the volume flow through the tight junction is from lumen to channel, and the fluid that enters the channel at the tight junction is hypotonic. The channel NaCl concentration declines near the tight junction at 0 mm Hg transmural pressure. This decline reflects the loss of NaCl by diffusion through the tight junction.

At both 0 and 20 mm Hg transmural pressure difference, volume flow rate increases nearly linearly with distance. The curve for 0 mm Hg has a slight upward concavity near the tight junction in the same region

where the NaCl concentration declines. The continuous increase of the volume flow rate arises from the failure of the net driving force on water to vanish, which is in turn due to the use of a uniform distribution of pumps along the channel. Other pump distributions can yield nonlinear volume flow curves and can permit equilibration of hydrostatic and osmotic pressures across the cell membrane in the vicinity of the basement membrane (vide infra).

The values for volume flow rate at a fractional distance of 1.0 are the values for reabsorption by the entire channel system. For the two transmural pressures shown in Fig. 4, the emergent flows differ by 1.03×10^{-12} ml/sec, while at the tight junction, the flows differ by only 0.61×10^{-12} ml/sec. For the choice of parameters used here, the response of the system to a change in transmural hydrostatic pressure is mediated in part by an alteration of the rate of fluid flow through the tight junction, and in part by an alteration of the rate of NaCl diffusion through the tight junction. The rate of fluid flow through the tight junction is proportional to the sum of the hydrostatic and effective osmotic forces acting across that boundary. Reducing interstitial hydrostatic pressure (increasing the transmural pressure difference) reduces channel hydrostatic pressure and so tends to increase fluid flow from lumen to channel. This effect serves to reduce channel NaCl concentration, so that diffusive NaCl flux through the tight junction is reduced. More NaCl is therefore available to exert an osmotic effect on the cell membrane bounding the channel. Thus, despite the fact that the channel NaCl concentration is less when the transmural pressure is 20 mm Hg than when the pressure is 0 mm Hg, the net driving force moving water across the cell membrane is actually greater with the transmural pressure of 20 mm Hg. Near $\lambda = 1$, the sum of the hydrostatic and osmotic pressures is 7.4 mm Hg at a transmural pressure difference of 20 mm Hg, but only 6.9 mm Hg with the transmural pressure at 0 mm Hg.

A striking feature of these results is that the osmotic and hydrostatic forces are of the same order of magnitude. The conventional view of forces governing water movement across cell membranes is that osmotic forces are larger than hydrostatic ones. Yet whenever we changed parameter values in an effort to raise the channel NaCl concentration, the channel hydrostatic pressure would rise to physiologically unreasonable levels, and the system would lose sensitivity to changes of transmural hydrostatic pressure in the range known to be effective with the proximal tubule. Clearly, the channel hydrostatic pressure rises under these circumstances because of the driving force on water movement across the cell

Table 1. Values of system variables obtained using the reference set of parameters

Transmural pressure (mm Hg)	Flow (ml/sec)	Emergent osmolality (osm)	Channel pressure (mm Hg)	Channel area (relative)
0	2.83×10^{-12}	0.301	16.2	0.63
10	3.35×10^{-12}	0.299	7.3	0.44
20	3.86×10^{-12}	0.298	− 1.6	0.28
30	4.34×10^{-12}	0.296	−10.6	0.15
40	4.80×10^{-12}	0.296	−19.7	0.08

membrane exerted by the high NaCl concentrations. But as channel hydrostatic pressure rises, changes of transmural hydrostatic pressure by some fixed amount, say 20 mm Hg, have a progressively smaller fractional effect on channel hydrostatic pressure. Our results suggest, therefore, that sensitivity of flow rate to the transmural hydrostatic pressure difference requires that the channel NaCl deviate only slightly from isotonic levels. Machen and Diamond [23] estimated NaCl concentrations in intercellular channels of rabbit gallbladder and concluded that the deviation from isotonicity, though real, was small.

Table 1 lists the values of certain system variables, computed with the reference parameter set. The rate of reabsorption varied nearly linearly with the transmural hydrostatic pressure difference; the sensitivity of flow to pressure was somewhat greater than the value reported by Spitzer and Windhager [29]. Emergent osmolality varied slightly, but remained within 2% of isotonicity. Channel hydrostatic pressure tracked interstitial pressure, always remaining higher than interstitial pressure. The relative cross-section area of the channel declined with increasing transmural hydrostatic pressure, because the change of channel hydrostatic pressure altered the hydrostatic pressure difference between the cell and the channel. At a transmural hydrostatic pressure difference of 0 mm Hg, channel pressure exceeded cell pressure, while at transmural differences of 10 mm Hg or greater, cell pressure exceeded channel pressure.

In the following sections, we shall discuss the sensitivity of the system to our choice of parameters and also to our assumptions regarding the geometry.

A. Parametric Sensitivity

In this section we shall discuss the effects on system performance of changing the values of the dimensionless parameters over a wide range,

usually four orders of magnitude. In all cases, we assume that the end membrane areas remain constant, and that the channel compliance is stiff ($\xi = 0.083$). For all the parameters except k_2, the pumping rate is assumed constant at 10^{-15} osmoles/sec; for k_2, the parameter value is assumed to change in response to changes in the pumping rate.

k_1: An increase in k_1 corresponds to an increase in the channel wall permeability relative to the axial diffusion permeability. When k_1 is small, little water enters from the cell, hence the channel fluid becomes hypertonic. The emergent fluid is hypertonic, since the hypertonicity of the channel fluid results in a large diffusive flux into the interstitium, and the convective flow is small compared to this diffusive flux. As k_1 increases, the channel fluid approaches isotonicity so that convective flow is large compared with diffusive flow, and a near isotonic reabsorbate results.

Table 2 shows how the system response changes when k_1 takes on values 0.01, 0.1, 2, and 3.0 times its reference value. When k_1 is small, the hypertonicity of the channel fluid results in high hydrostatic pressures.

When k_1 becomes very large (greater than about 40), the solution becomes unstable near the ends of the channel. The extremely high wall permeability leads to hydraulic equilibrium along the channel, while the permeabilities of the end membranes lead to solute concentrations not at hydraulic equilibrium with the cell. These conditions are not compatible with the model assumptions of no radial concentration gradients and uniform equivalent end membranes. Thus, for high values of k_1, the model of the end processes would have to be recast as a partial differential equation system. Although this is computationally feasible, its implementation would require considerably more morphological data than are now available. We shall thus limit the discussion to those results shown to be compatible with our model.

k_2: The changes in the system operation as k_2 changes are shown in Table 3. The value of k_2 is proportional to the solute pumping rate. With small to moderate increases of k_2 over the reference value, water flow through the cell wall can increase sufficiently so that the emergent fluid remains isotonic. When k_2 becomes very large, however, the channel fluid becomes hypertonic, both channel pressure and emergent osmolality increase markedly, and the sensitivity of flow rate to transmural hydrostatic pressure declines. The channel fluid becomes hypertonic at high values of k_2 because convective flow is insufficient to sweep out all the NaCl being pumped; the channel concentration rises until additional diffusive flow develops across the basement membrane and tight junction to ensure mass balance. The reabsorbate becomes hypertonic because of the aug-

Table 2. Sensitivity of system performance to variation of k_1, the dimensionless hydraulic conductance of the channel wall[a]

k_1	0.12		1.2		12.0		24.0		36.0	
Transmural hydrostatic pressure difference, mm Hg	0	20	0	20	0	20	0	20	0	20
Reabsorptive flow rate (ml/sec) $\times 10^{12}$	0.222	0.268	1.37	1.68	2.83	3.86	3.01	4.56	3.09	5.14
Ratio of reabsorptive flow rates[b]	1.21		1.23		1.36		1.52		1.67	
Emergent osmolality, osmolar	0.589	0.534	0.329	0.321	0.301	0.298	0.300	0.298	0.299	0.298
Channel hydrostatic pressure, mm Hg	58.8	48.8	40.0	26.9	16.2	−1.6	13.3	−5.1	12.3	−6.3
Channel cross-section area, fraction of maximum	0.98	0.96	0.92	0.80	0.63	0.28	0.57	0.22	0.55	0.21

[a] The values for the other system parameters are those of the reference set listed in the text. Solute pumping rate, N_0, $= 10^{-15}$ osmoles/sec for all cases.
[b] Calculated as the reabsorptive flow rate at transmural pressure of 20 mm Hg divided by the flow rate at transmural pressure of 0 mm Hg.

Table 3. Sensitivity of system performance to variation of k_2, the dimensionless pumping rate[a]

k_2	0.0003		0.003		0.03		0.3		3.0	
Solute pumping rate, osmoles/sec	10^{-17}		10^{-16}		10^{-15}		10^{-14}		10^{-13}	
Transmural hydrostatic pressure difference, mm Hg	0	20	0	20	0	20	0	20	0	20
Reabsorptive flow rate (ml/sec) $\times 10^{12}$	0.0284	1.01	0.284	1.27	2.83	3.86	27.9	29.0	257.0	258.0
Ratio of reabsorptive flow rates[b]	35.70		4.49		1.36		1.04		1.01	
Emergent osmolatity, osmolar	0.301	0.288	0.301	0.291	0.301	0.298	0.305	0.304	0.336	0.335
Channel hydrostatic pressure, mm Hg	10.1	−7.9	10.6	−7.3	16.2	−1.6	71.2	53.5	574.0	557.0
Channel cross-section area, fraction of maximum	0.50	0.18	0.51	0.19	0.63	0.28	0.994	0.974	0.999	0.999

[a] The values for the other system parameters are those of the reference set listed in the text.
[b] Calculated as the reabsorptive flow rate at transmural pressure of 20 mm Hg divided by the flow rate at transmural pressure of 0 mm Hg.

mented diffusion of NaCl across the basement membrane, and also because the concentration near the basement membrane is hypertonic, so that even the convective flow becomes hypertonic. The channel pressure rises because of the increased rate of fluid flow into the channel, and because of the limit to the dilatation of the channel imposed by the compliance. The loss of sensitivity to variations of transmural pressure when k_2 is high can be attributed to the high channel hydrostatic pressure. If the channel pressure is of the order of several hundred mm Hg, variations of transmural pressure within the physiological range of interest will induce trivial fractional changes in the channel pressure, and the performance of the system will not be altered significantly. Only when the channel pressure has approximately the same value as the hydrostatic pressures in the structures that border the channel will transmural pressure exert significant control over the rate of fluid reabsorption.

k_3: The value of k_3 is proportional to the value of the basement membrane hydraulic permeability. As shown in Table 4, when k_3 is decreased, fluid encounters greater resistance as it flows into the interstitium, and channel pressure rises. The rise in channel pressure opposes water movement from the cell, so that the rate of fluid reabsorption falls, channel NaCl concentration rises, and the reabsorbate becomes hypertonic. If the value of k_3 is above approximately 0.5, however, the reabsorbate is very nearly isotonic. Increasing k_3, in reducing the outflow resistance, allows the rate of fluid flow into the interstitium to increase modestly. Major increases of k_3 have little effect on the performance of the system.

k_4: Changes in k_4 reflect changes in the tight junction hydraulic permeability; the effects are shown in Table 5. When k_4 is reduced from its reference value, water flow through the tight junction declines. When the transmural hydrostatic pressure difference is 0 mm Hg, the fluid flow is from channel to lumen; reducing k_4 therefore forces the flow that would have crossed the tight junction to move instead across the basement membrane, so that total reabsorptive flow increases. When the transmural pressure difference is 20 mm Hg, the flow at the tight junction is from lumen to channel; reducing k_4 therefore eliminates this flow and the reabsorptive rate declines. Sensitivity to variation of transmural hydrostatic pressure declines as k_4 is reduced, because of the lost ability of the system to move water through the tight junction. Some sensitivity is retained, however, because the diffusion of NaCl through the tight junction continues despite the reduction of fluid flow through the tight junction.

When k_4 becomes larger, fluid flow through the tight junction becomes more sensitive to variations of transmural hydrostatic pressure. When

Table 4. Sensitivity of system performance to variation of k_3, the dimensionless basement membrane hydraulic permeability[a]

k_3	0.01		0.1		1.0		10.0		100.0	
Transmural hydrostatic pressure difference, mm Hg	0	20	0	20	0	20	0	20	0	20
Reabsorptive flow rate (ml/sec) $\times 10^{12}$	0.231	0.316	1.40	1.91	2.83	3.86	3.15	4.27	3.18	4.31
Ratio of reabsorptive flow rates[b]	1.37		1.37		1.36		1.35		1.35	
Emergent osmolatity, osmolar	0.440	0.400	0.315	0.308	0.301	0.298	0.300	0.297	0.300	0.297
Channel hydrostatic pressure, mm Hg	60.4	58.9	40.5	31.7	16.2	−1.6	10.7	−9.1	10.1	−10.0
Channel cross-section area, fraction of maximum	0.985	0.983	0.92	0.86	0.63	0.28	0.52	0.17	0.50	0.16

[a] The values for the other system parameters are those of the reference set listed in the text. Solute pumping rate, $N_0 = 10^{-15}$ osmoles/sec for all cases.
[b] Calculated as the reabsorptive flow rate at transmural pressure of 20 mm Hg divided by the flow rate at transmural pressure of 0 mm Hg.

Table 5. Sensitivity of system performance to variations of k_4, the dimensionless tight junction hydraulic permeability[a]

k_4	0.001		0.01		0.1		1.0		10.0	
Transmural hydrostatic pressure difference, mm Hg	0	20	0	20	0	20	0	20	0	20
Reabsorptive flow rate (ml/sec) $\times 10^{12}$	2.93	3.49	2.92	3.53	2.83	3.86	2.31	5.52	1.73	7.30
Ratio of reabsorptive flow rates[b]	1.19		1.21		1.36		2.39		4.21	
Emergent osmolality, osmolar	0.301	0.298	0.301	0.298	0.301	0.298	0.302	0.298	0.302	0.299
Channel hydrostatic pressure, mm Hg	16.4	−2.4	16.4	−2.4	16.2	−1.6	15.1	2.0	13.8	5.9
Channel cross-section area, fraction of maximum	0.63	0.26	0.63	0.26	0.63	0.28	0.60	0.34	0.58	0.41

[a] The values for the other system parameters are those of the reference set listed in the text. Solute pumping rate, $N_{0_s} = 10^{-15}$ osmoles/sec for all cases.

[b] Calculated as the reabsorptive flow rate at transmural pressure of 20 mm Hg divided by the flow rate at transmural pressure of 0 mm Hg.

the transmural hydrostatic pressure difference is 0 mm Hg, the magnitude of the fluid flow from channel to lumen is increased, so less fluid is available for the formation of the reabsorbate. When the interstitial hydrostatic pressure declines, the flow is from lumen to channel; when k_4 is large, this flow is large, and since the tight junction flow is added to the fluid in the channel, the reabsorptive rate increases. Thus, the sensitivity of reabsorptive flow depends heavily on the value of k_4, over a range of values spanning four orders of magnitude. The criterion we used for selecting the reference value was that it yielded a reasonable fit to the limited data available.

k_5: A change in the solute permeability of the basement membrane has little effect on the system operation, as can be seen from Table 6, until k_5 becomes large (on the order of 0.5); at that point, emergent osmolality becomes anisotonic. The reason for this effect is that the concentration of NaCl near the basement membrane need not be strictly at isotonic levels. When k_5 takes on very high values, diffusive flow across the basement membrane increases to numerically significant levels, and determines emergent osmolality. Provided that k_5 is sufficiently small, the system is insensitive to the exact value chosen for the parameter.

k_6: The NaCl permeability of the tight junction is proportional to k_6. If k_6 is small, there can be little back diffusion through the tight junction, and solute pumped into the channel can leave only by crossing the basement membrane. Thus, as shown in Table 7, reducing k_6 when the transmural hydrostatic pressure difference is 0 mm Hg increases the rate of fluid reabsorption because NaCl is now unable to diffuse from channel to lumen. In contrast, when the transmural pressure difference is 20 mm Hg, the concentration gradient across the tight junction favors NaCl diffusion into the channel; reducing k_6 eliminates this source of NaCl, and less is available to extract water from the cells to form the reabsorbate. The overall effect of reducing k_6 is to reduce the sensitivity of the system to changes of the transmural hydrostatic pressure difference. Increasing k_6, on the other hand, exaggerates the diffusive flux, whatever its direction, and increases the sensitivity to changes of transmural pressure. Since there is now abundant evidence that NaCl crosses the tight junction [3, 9, 11–14, 17, 27, 30], k_6 must be assigned some nonzero value. The value we selected provides a reasonable fit to the data available.

k_7: Increasing the tight junction reflection coefficient has the effect of reducing the sensitivity to transmural pressure changes. The magnitude of this effect is shown in Table 8, where k_7 is varied from 0.01 to 0.99. As k_7 increases, the effective osmotic pressure across the tight junction

Table 6. Sensitivity of system performance to variation of k_5, the dimensionless basement membrane solute permeability[a]

k_5	0.0005		0.005		0.05		0.5		5.0	
Transmural hydrostatic pressure difference, mm Hg	0	20	0	20	0	20	0	20	0	20
Reabsorptive flow rate (ml/sec) $\times 10^{12}$	2.85	3.85	2.85	3.85	2.83	3.86	2.66	3.90	2.14	4.02
Ratio of reabsorptive flow rates[b]	1.35		1.35		1.36		1.47		1.88	
Emergent osmolality, osmolar	0.299	0.298	0.299	0.298	0.301	0.298	0.323	0.294	0.411	0.284
Channel hydrostatic pressure, mm Hg	16.3	−1.7	16.3	−1.7	16.2	−1.6	15.8	−1.5	14.7	−1.3
Channel cross-section area, fraction of maximum	0.63	0.27	0.63	0.27	0.63	0.28	0.62	0.28	0.60	0.28

[a] The values for the other system parameters are those of the reference set listed in the text. Solute pumping rate, $N_0, = 10^{-15}$ osmoles/sec for all cases.

[b] Calculated as the reabsorptive flow rate at transmural pressure of 20 mm Hg divided by the flow rate at transmural pressure of 0 mm Hg.

Table 7. Sensitivity of system performance to variations in k_6, the dimensionless tight junction solute permeability[a]

k_6	0.01		0.1		1.0		10.0		100.0	
Transmural hydrostatic pressure difference, mm Hg	0	20	0	20	0	20	0	20	0	20
Reabsorptive flow rate (ml/sec) $\times 10^{12}$	3.23	3.69	3.18	3.71	2.83	3.86	2.17	4.07	1.97	4.13
Ratio of reabsorptive flow rates[b]	1.14		1.17		1.36		1.87		2.09	
Emergent osmolality, osmolar	0.301	0.298	0.301	0.298	0.301	0.298	0.302	0.298	0.302	0.298
Channel hydrostatic pressure, mm Hg	17.1	−2.0	17.0	−2.0	16.2	−1.6	14.8	−1.2	14.3	−1.0
Channel cross-section area, fraction of maximum	0.64	0.27	0.64	0.27	0.63	0.28	0.60	0.28	0.59	0.29

[a] The values for the other system parameters are those of the reference set listed in the text. Solute pumping rate, $N_0, = 10^{-15}$ osmoles/sec for all cases.

[b] Calculated as the reabsorptive flow rate at transmural pressure of 20 mm Hg divided by the flow rate at transmural pressure of 0 mm Hg.

Table 8. Sensitivity of system performance to variations in k_7, the tight junction NaCl reflection coefficient[a]

k_7	0.01		0.1		0.3		0.7		0.99	
Transmural hydrostatic pressure difference, mm Hg	0	20	0	20	0	20	0	20	0	20
Reabsorptive flow rate (ml/sec) $\times 10^{12}$	2.69	3.98	2.73	3.95	2.83	3.86	2.96	3.62	2.97	3.59
Ratio of reabsorptive flow rates[b]	1.48		1.44		1.36		1.22		1.21	
Emergent osmolality, osmolar	0.302	0.298	0.302	0.298	0.301	0.298	0.301	0.298	0.301	0.298
Channel hydrostatic pressure, mm Hg	15.9	−1.4	16.0	−1.5	16.2	−1.6	16.5	−2.2	16.5	−2.2
Channel cross-section area, fraction of maximum	0.62	0.28	0.62	0.28	0.63	0.28	0.63	0.27	0.63	0.27

[a] The values for the other system parameters are those of the reference set listed in the text. Solute pumping rate, $N_0, = 10^{-15}$ osmoles/sec for all cases.

[b] Calculated as the reabsorptive flow rate at transmural pressure of 20 mm Hg divided by the flow rate at transmural pressure of 0 mm Hg.

increases. Thus, when k_7 is 0.1 and at 0 mm Hg transmural pressure, net water flux across the tight junction is from channel to lumen; when k_7 is 0.9, the water flux is in the opposite direction. With the reference set of parameters, the sensitivity of reabsorptive flow to transmural hydrostatic pressure depends in part on the water flux across the tight junction. As k_7 increases, the hydrostatic pressure difference across the tight junction becomes a smaller fraction of the total driving force on the water flux, and the sensitivity declines. Conversely, when k_7 is near zero, the effective osmotic pressure difference across the tight junction is small, the hydrostatic pressure difference is the principal determinant of water flow through the tight junction, and the sensitivity to transmural pressure is enhanced. As with the other tight junction parameters, the value of k_7 has no significant effect on emergent osmolality.

k_8: The value of the basement membrane reflection coefficient has very little effect on the reabsorption rate, but it is a principal factor in determining the osmolality of the reabsorbate. If k_8 is large (greater than about 0.05), the reabsorbate is significantly hypotonic. These results are shown in Table 9.

B. End Membrane Conditions

In the derivation of the equations, we assumed that the area of both the basement membrane and the tight junction membrane remain constant. In this section, we examine the consequences of allowing these areas to be variable. For the variable basement membrane, the dimensionless boundary value equations corresponding to Eqs. (35) and (36) are

$$\alpha(0)=k_4 r[\Phi_L-\Phi+k_7\gamma(0)] \tag{42}$$

and

$$\frac{k_1}{r}\alpha(0)\left[k_7+(1+k_7)\frac{\gamma(0)}{2}\right]-\beta(0)=-k_6\gamma(0). \tag{43}$$

For the variable tight junction, the equations are

$$\alpha(1)=k_3 r[\Phi-\Phi_{IS}-k_8\gamma(1)] \tag{44}$$

and

$$\frac{k_1}{r}\alpha(1)\left[k_8+(1+k_8)\frac{\gamma(1)}{2}\right]-\beta(1)=k_5\gamma(1). \tag{45}$$

Table 9. Sensitivity of system performance to variations in k_8, the basement membrane NaCl reflection coefficient[a]

k_8	0.0001		0.001		0.005		0.05		0.10	
Transmural hydrostatic pressure difference, mm Hg	0	20	0	20	0	20	0	20	0	20
Reabsorptive flow rate (ml/sec) $\times 10^{12}$	2.82	3.84	2.82	3.84	2.83	3.86	2.90	4.02	2.98	4.19
Ratio of reabsorptive flow rates[b]	1.36		1.36		1.36		1.38		1.40	
Emergent osmolality, osmolar	0.303	0.299	0.303	0.299	0.301	0.298	0.288	0.285	0.274	0.270
Channel hydrostatic pressure, mm Hg	16.1	−1.7	16.1	−1.7	16.2	−1.6	17.1	−1.3	18.3	−0.7
Channel cross-section area, fraction of maximum	0.62	0.28	0.62	0.28	0.63	0.28	0.64	0.28	0.67	0.29

[a] The values for the other system parameters are those of the reference set listed in the text. Solute pumping rate, $N_0, = 10^{-15}$ osmoles/sec for all cases.

[b] Calculated as the reabsorptive flow rate at transmural pressure of 20 mm Hg divided by the flow rate at transmural pressure of 0 mm Hg.

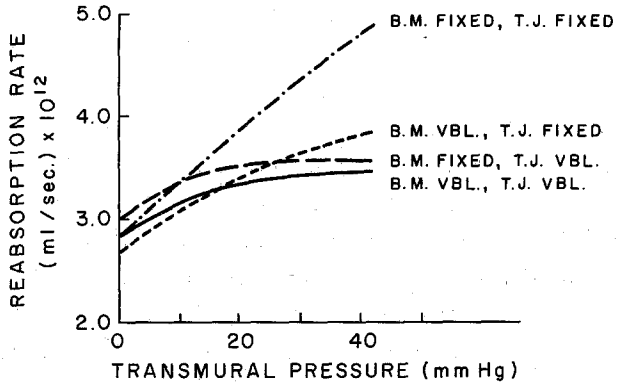

Fig. 5. Emergent flow as a function of the transmural pressure difference for all four combinations of end membrane geometries. B.M. = basement membrane, T.J. = tight junction, Vbl. = variable

In all cases, the dimensionless parameter values, compliance function, pumping rate, and pump distribution function are unchanged from the reference case. Fig. 5 shows the flow as a function of transmural pressure for all four combinations of end conditions. The Figure shows that when the tight junction is variable, the flow seems to approach a saturation value. This is due to the reduction in the tight junction area as the channel area decreases with increased transmural pressure. The reduced area thus reduces the solute and water fluxes through the tight junction, hence flow modulation is more difficult. At very small areas, this modulating flux is effectively cut off.

Allowing the basement membrane area to vary with channel area has a similar effect, though not so pronounced. Reducing the area has the effect of reducing the permeability of the basement membrane relative to the fixed area case, hence the flow is reduced.

The choice of geometry of the tight junction has little effect on the emergent osmolality. When the basement membrane is held fixed, the emergent osmolality ranges from 0.301 at 0 mm Hg transmural pressure, to 0.296 at 50 mm Hg transmural pressure. When the basement membrane is variable, the same pressure variation leads to a change in osmolality from 0.301 to 0.298.

There has been some speculation that the mechanism of flow modulation by hydrostatic pressure is a variation in tight junction solute permeability induced by changes in cross-section area of the channel [17]. Our results show that the tight junction need not vary its permeability to account for the known behavior of this system. Moreover, given the

assumptions of our model (constant pumping rate, symmetric compliance function, constant channel circumference, etc.) we conclude that the tight junction geometry should remain constant to provide the type of flow modulation observed by Spitzer and Windhager [29]. However, no such conclusion can be reached regarding the basement membrane. Although some curvature of the response function is apparent, the curve does not differ radically from the limited experimental data available. Thus, it is still possible that the actual system responds to alterations of transmural hydrostatic pressure with a variation of the basement membrane area. The choice of fixed basement membrane area as the reference case is therefore arbitrary.

C. Pump Distribution

We initially assumed that the pumps were distributed uniformly over the length of the channel. We tested three other distributions to determine whether the choice of a distribution function influenced the results. First, we assumed that the pump density decreased uniformly from the tight junction to the basement membrane; second, we assumed that the density decreased parabolically from the tight junction to the midpoint of the channel, with no pumps on the second half; third, we distributed all the pumps uniformly over the first 10% of the length, following the model of Diamond and Bossert [10]. The four distributions are displayed in Fig. 6.

Shown in Fig. 7 are the concentration profiles along the channel for each distribution, for a transmural pressure difference of 0 mm Hg. The system performance variables for all four distributions are shown in Table 10. These values show that changing the distribution only mildly affects the operation of the system. Such differences as do exist are due to increases in the diffusive backflux into the lumen as a result of moving the pumps closer to the tight junction.

Fig. 8 shows the concentration profiles at a transmural pressure of 20 mm Hg. In this case, all the distributions result in a hypotonic channel fluid near the serosal end of the channel. The cases where the pumps are concentrated near the luminal end have a higher concentration near the tight junction, hence diffusive backflux is greater than for the case of uniform distribution. This results in a higher solute backflux into the lumen. The greater hypotonicity results from the fact that no pumps exist on the later portion of the channel in two of the cases; thus, the system can reach hydraulic equilibrium with the cell. When pumps are

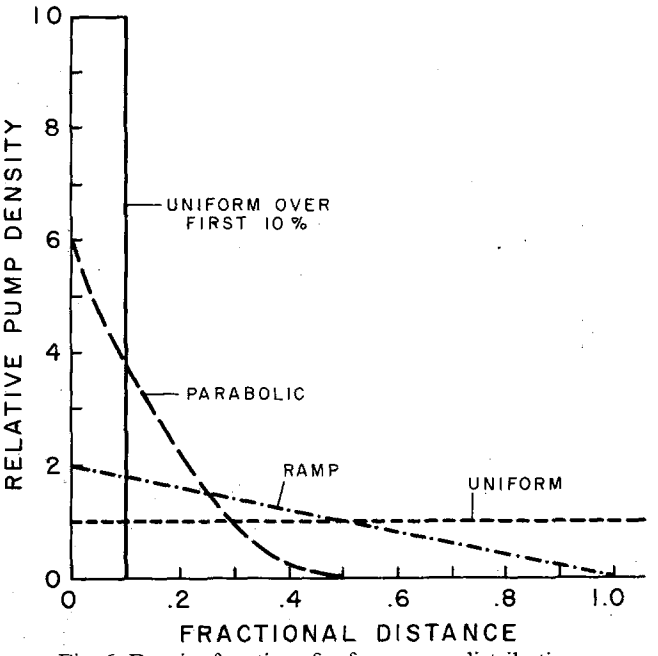

Fig. 6. Density functions for four pump distributions

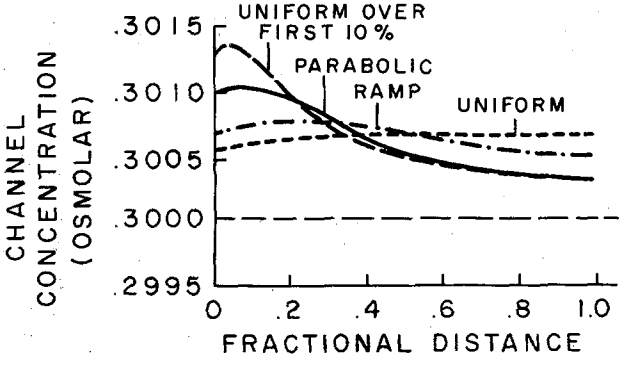

Fig. 7. Concentration profiles for four pump distribution functions. Transmural pressure difference = 0 mm Hg

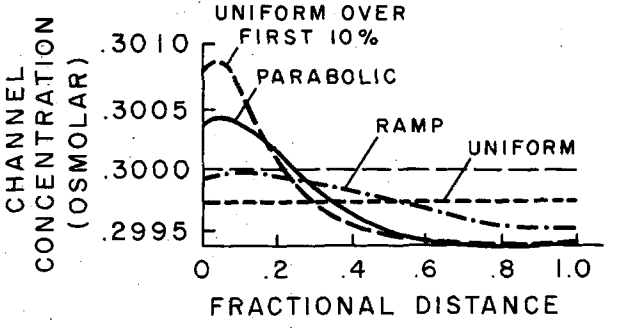

Fig. 8. Concentration profiles for four pump distribution functions. Transmural pressure difference = 20 mm Hg

Table 10. Sensitivity of system performance to pump distribution function[a]

	Pump distribution[b]							
	Uniform		Ramp		Parabolic		Uniform over first 10%	
Transmural hydrostatic pressure, mm Hg	0	20	0	20	0	20	0	20
Reabsorptive flow rate, ml/sec × 10^{12}	2.83	3.86	2.81	3.84	2.75	3.73	2.95	3.88
Ratio of reabsorptive flow rates[c]	1.36		1.36		1.36		1.32	
Emergent osmolality, osmolar	0.301	0.298	0.301	0.297	0.300	0.297	0.300	0.297
Channel hydrostatic pressure, mm Hg	16.2	−1.6	16.2	−1.7	16.1	−1.7	16.2	−1.6
Channel cross-section area, fraction of maximum	0.63	0.28	0.63	0.27	0.62	0.27	0.63	0.28

[a] The values for the system parameters are those of the reference set listed in the text. Solute pumping rate, N_0, $= 10^{-15}$ osmoles/sec for all cases.
[b] Distribution of pumps along channel; terms are defined in text.
[c] Calculated as the reabsorptive flow rate at transmural pressure of 20 mm Hg divided by the flow rate at transmural pressure of 0 mm Hg.

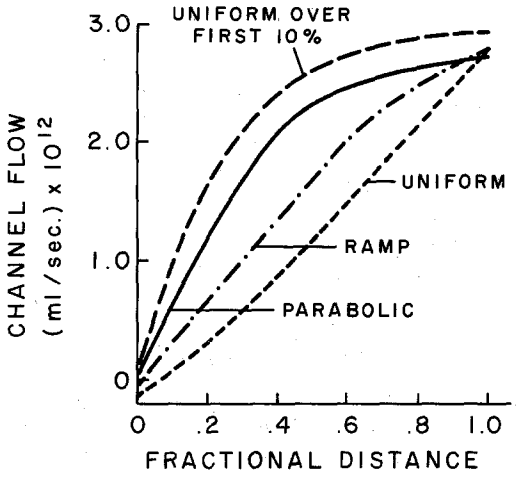

Fig. 9. Flow profiles for four pump distribution functions. Transmural pressure difference = 0 mm Hg

located all along the channel, equilibrium is not reached, and the osmolality is somewhat higher.

Fig. 9 shows the flow profiles over the length of the channel, for zero transmural pressure. The rate of change of flow is proportional to the local concentration difference between channel and cell; thus the flow curves follow directly from the concentration curves of Figs. 7 and 8.

D. Compliance

The model behavior was examined for various values of the compliance parameter ξ. Three values were used: the standard value, 0.083, an extremely stiff value, 0.01, and a very compliant value, 0.44. The system operation changed negligibly over this range; the lack of sensitivity is due to the fact that the flow is determined by the channel pressure. The area adjusts by the particular compliance function being used.

We also tested the compliance function using a variable basement membrane. Fig. 10 shows the response curves for three values of ξ. As the channel becomes softer (ξ becomes larger), the response curve departs more from linearity. When the channel compliance is very soft, the channel is either nearly completely open or nearly closed; there is only a very small pressure range where the area occupies intermediate values. In this case, the channel pressure is relatively insensitive to transmural pressure.

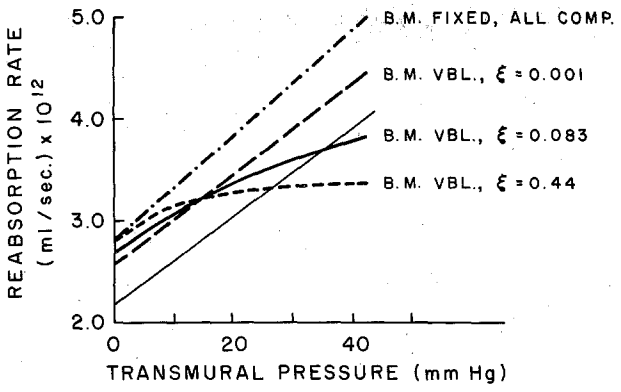

Fig. 10. Emergent flow for two basement membrane geometries and various compliance functions. The tight junction area is fixed in all cases. B.M. = basement membrane, COMP. = compliance, VBL. = variable

This insensitivity is also reflected in the channel solute concentration, which changes little; thus, the reabsorption rate also becomes insensitive to transmural pressure. On the other hand, when the channel is extremely stiff, there is very little change in area with transmural pressure, but the channel pressure changes nearly as much as the transmural pressure, and the system responds very well to changes in transmural pressure. However, the channel area remains virtually constant, and micrographic data for different transport rates indicate that significant area changes do occur, at least in the jejunum [11]. Hence, we would reject the very stiff compliance function in conjunction with the variable basement membrane. For the case of fixed basement membrane area, the insensitivity of the response function to the compliance curve permits no precise estimation of ξ. In view of the number of parameters in this model, the fact that the performance is insensitive to one of them is to be counted as a positive advantage.

E. Cell Pressure

In our original analysis, we assumed that the cell pressure would remain constant and equal to the lumen pressure for all values of interstitial pressure. However, the cell itself will be a reactive element of the system, so we tested the effect of a variable cell pressure by allowing the cell hydrostatic pressure to equal the arithmetic mean of the lumen pressure and the channel pressure. Table 11 shows the resulting values of flow, emergent osmolality, channel pressure, and channel area for this configuration and for the reference case.

Table 11. Sensitivity of system performance to assuming cell hydrostatic pressure fixed or variable

Transmural pressure (mm Hg)	Flow (ml/sec) $\times 10^{-12}$		Emergent osmolality		Channel pressure (mm Hg)		Relative channel area	
	Variable	Fixed	Variable	Fixed	Variable	Fixed	Variable	Fixed
0	2.89	2.83	0.301	0.301	16.3	16.2	0.57	0.63
10	3.32	3.35	0.300	0.299	7.2	7.3	0.47	0.44
20	3.74	3.86	0.299	0.298	− 1.9	− 1.6	0.38	0.28
30	4.17	4.34	0.298	0.296	−11.0	−10.6	0.30	0.15
40	4.59	4.80	0.297	0.296	−20.1	−19.7	0.22	0.08

In the case of a variable cell pressure, there is little change in the channel pressure, but a significant change in the channel area. The decreased sensitivity of area results from the decrease in the pressure difference between cell and channel compared to the fixed cell pressure case.

A further consequence of this decreased cell-channel pressure difference is the reduced sensitivity of emergent osmolality to decreases in the interstitial pressure. When the cell pressure decreases along with the channel pressure, the anisotonicity of the channel fluid is less than in the fixed cell pressure case. Thus, the convective flux is more nearly isotonic, and the diffusive flux is reduced.

The response of this system is very nearly linear, but the sensitivity of flow to changes in transmural pressure is somewhat lower than that in the fixed cell pressure case. In the fixed case, changing transmural pressure from 0 to 20 mm Hg results in a 36 percent increase in flow; when the cell pressure is allowed to vary, only a 29 percent increase occurs. In general, the degree to which the cell pressure changes with changes in interstitial pressure has relatively little influence on the operation of the system.

Discussion

There are seven experimentally established facts about the behavior of the tight junction-intercellular channel complex in the proximal tubule and similar epithelia that are useful in formulating our model or in judging its fidelity. These are:

1. The reabsorptive rate can be reasonably well estimated under normal circumstances [15]. This rate was used to provide an estimate of k_2, which

is proportional to the rate of active transport, since the isotonicity of the reabsorbate creates a direct dependence of the volume rate of reabsorption on the rate of active transport.

2. The reabsorbate is isotonic under every experimental circumstance thus far examined [20, 34, 37]. In the proximal tubule, where roughly two-thirds of the glomerular filtrate is reabsorbed, the tubular fluid has never been found to be anisotonic, a fact that implies that an isotonic fluid has been reabsorbed from the isotonic filtrate. The experimental technique used to establish this fact has been measurement of the freezing point depression. These measurement techniques, as they are practiced in renal micropuncture laboratories, have an error of ± 2–3%. Regardless of the choice of pump distribution and other parameter values used, there was some dependence of reabsorbate tonicity on reabsorption rate. The range of computed tonicities was within the limits of uncertainty of the measurement methods, however, so that the model conforms to the known behavior of the system. The dependence of reabsorbate tonicity on reabsorptive rate arises from the variation of channel hydrostatic pressure with reabsorptive rate. In general, any change in the system that raises channel pressure leads to an increase in reabsorbate tonicity.

3. Variations in the transmural hydrostatic pressure difference, usually imposed by changing the protein concentration in plasma perfusing the peritubular capillaries, cause changes in the rate of isotonic fluid variations. Increased transmural pressure enhances the rate of reabsorption, while decreased transmural pressure decreases reabsorption [4–8, 11, 16, 17, 21, 24, 29]. The model results reflect these changes. Since reabsorptive rate and transmural pressure differences have not been measured simultaneously, it is not possible to compare the responsiveness of the model with that of a real epithelium. We have assumed that there is a linear relationship between peritubular plasma oncotic pressure and interstitial pressure, and have sought to match the performance of the model to the data of Spitzer and Windhager [29], who perfused peritubular capillaries with synthetic plasmas and measured the effects on fluid reabsorption. The relationships between capillary variables and interstitial pressure may be nonlinear, but we have elected to ignore this possibility in the absence of specific indications to the contrary. Thus, because Spitzer and Windhager [29] found a linear relationship between plasma oncotic pressure and reabsorption rate, the model was tuned to yield a similar relationship. The feature that permits this linearity is the constancy of the permeability-surface area product of the tight junction membrane. Future experiments may reveal a more complex relationship between trans-

mural pressure and reabsorption rate; for the present, the model suggests rejection of the notion that the properties of the tight junction change in response to variations of transmural pressure.

4. Sugar molecules as large as sucrose and raffinose pass through the tight junction [1, 15, 22, 30]. We interpret this result to mean that water can also cross the tight junction, so that the value of k_4, which is proportional to the water permeability of the junction, is not zero. A consequence of assigning some positive value to k_4 is that flow of water through the tight junction becomes a significant phenomenon in the modulation of reabsorption by transmural pressure.

5. The tight junction provides a pathway for the passage of NaCl. This assumption, which is a major departure of our model from that of Diamond and Bossert [10] is supported by a good deal of electrophysiological evidence in proximal tubule of the rat [27] and of *Necturus* [3, 30], in the small intestine [11], and in the gallbladder [13]. This evidence supports the decision to assign a nonzero value to k_6, the dimensionless NaCl permeability of the tight junction. It should be understood that the modulation of the diffusive flux of NaCl through this pathway is an absolute requirement for maintaining near isotonic reabsorption while transmural pressure is being manipulated. With a constant pumping rate, isotonic reabsorption is compatible with a variable rate of reabsorption only if the NaCl flux through the tight junction adapts to the transmural pressure difference. In our simulations, the direction of this flux can change from channel to lumen at low flow rates to lumen to channel at high flow rates. Whether the flux changes direction in life remains to be determined, but that it must change in magnitude to ensure isotonicity seems certain.

6. The cross-section area of the channel increases with decreasing transmural pressure in the model, because reducing the transmural pressure difference diminishes the pressure difference driving fluid from the channel into the interstitium, and the channel therefore distends. Electronmicrographic evidence supports this finding for the small intestine [11], but is inconclusive in the proximal tubule [7, 31]. The permeability of the proximal tubule tight junction-channel complex to sugars [1, 22] and the electrical conductivity [3, 27, 30] increase with decreasing transmural pressure. These changes have been interpreted as reflecting dilatation of the channel. The model results are consistent with such interpretations; a dilated channel will offer less diffusive resistance to sugars than a narrow channel, and a dilated channel with an elevated NaCl concentration will be more conductive than a narrow channel with a lower NaCl con-

centration. The simulations show that the dilatation is governed to a large extent by the value of the compliance parameter, while the performance of the system is otherwise indifferent to this choice. Thus, the failure to find significant variation of channel area with transmural pressure is not critical in judging the general validity of the hypothesis that flow modulation is carried out in the tight junction-lateral intercellular channel complex. The results suggesting variations in channel cross-section area have been important in the development of present thinking about this system. So far as we can judge, however, this variation is only a consequence of the hydrostatic pressure difference across the cell membrane, and, at least in the steady state, has no important effects on the operation of the system.

7. The cross-section area of the channel decreases with decreasing pump rates. This phenomenon was first noted by Tormey and Diamond [32]. In our simulations, reductions of k_2, the dimensionless pumping rate, led to smaller channel cross-section areas, as shown in Table 3. While these changes are not as extreme as those reported by Tormey and Diamond, the use of a softer compliance could have made them so.

Because of the fact that the number of parameters exceeds the number of quantitative experimental results, no unique solution can be found. The sensitivity studies reveal that for certain of the parameters, namely k_1, k_3, k_5, k_8 and ξ, there is a range of values that enables the system to behave in a manner consistent with experimental results. For each of these parameters, any value within this range will suffice. The value of k_2 determines the rate of reabsorption which is to be modulated by the transmural pressure difference, and which is therefore known.

Three parameters change system performance over the entire range of values studied – four orders of magnitude for k_4 and k_6, and 0.01 to 0.99 for k_7. The exact value of each of these parameters matters very much to the system, but there are no data that would permit assignment of precise values. These three parameters constitute the set of phenomenological coefficients for the tight junction membrane. From experimental results, we know that NaCl diffuses through the tight junction, and from the simulations it would appear that this diffusive flux must be altered if the rate of isotonic reabsorption is to be modulated by transmural pressure, so that k_6 cannot be zero.

Whether there is a water flux across the tight junction remains to be determined. The permeation of sugar molecules suggests there could be significant water permeability although the magnitude of the water permeability and of the reflection coefficient can only be estimated from

such data with the help of specific physical models under the assumption that tight junction movement is rate governing. As discussed above, there is some evidence that the channel and the basement membrane provide some resistance to the flow of these materials. When the lumen of the proximal tubule is perfused with solutions containing protein, the reabsorption rate is not affected. This result suggests either that the water permeability of the junction is nearly zero, certainly a real possibility, or that the tight junction reflection coefficient for protein is nearly zero, an unlikely possibility. The difficulty with the interpretation of experiments in which proteins are brought in direct contact with the cell membrane is that Donnan effects may alter cell function directly. Since we have held k_2 constant, the model could not predict such an effect. Thus, we cannot answer the question of whether there is a water flux at the tight junction.

The question of tight junction water flow is important because the results of our simulations suggest that a water flux can have a significant amplifying effect on the diffusive flux of NaCl. When water flux is from channel to lumen, as with a 0 mm Hg transmural pressure difference, the tight junction water flux raises the channel NaCl concentration which increases the diffusive backflux. Reversal of the water flux, as can be produced by increasing the transmural pressure difference, lowers the channel NaCl concentration below isotonic levels, so that the diffusive flux is from lumen to channel. If the tight junction water flux is eliminated by reducing the tight junction water permeability, the NaCl concentration of the channel still rises with diminished transmural pressure, and vice versa, but the excursions of the NaCl concentration are less than when water flows across the tight junction, and the sensitivity of reabsorption rate to transmural pressure is therefore diminished.

The results of our simulations provide yet another reason for wanting to determine the magnitude of the tight junction water flux. Table 6 shows that the basement membrane solute permeability must remain below some bound if reabsorption is to remain near isotonic. As shown in Fig. 3, the NaCl concentration in the channel varies with transmural hydrostatic pressure, creating a concentration gradient across the basement membrane. If the diffusive flux is large relative to the convective flux, reabsorption will not be isotonic for most values of transmural pressure. In order to provide sensitivity of reabsorption to transmural hydrostatic pressure, we assigned a value to the tight junction NaCl permeability that, as it happens, is 20 times the basement membrane permeability. The surface area of the basement membrane through which NaCl and water flow

is undoubtedly larger than the corresponding surface area of the tight junction. The relationship between the surface areas of the two structures suggests that the tight junction should have the lesser of the two permeabilities, but factors other than cross-sectional area can obviously determine the permeability of a structure.

Even if both tight junction and basement membrane are simple neutral channels, with a NaCl permeability ratio equal to the area ratio, it is still possible to have the model meet the performance criteria of isotonicity and pressure sensitivity by increasing the tight junction water permeability. For example, if the tight junction NaCl permeability is reduced to the same value as the corresponding basement membrane parameter, and the tight junction water permeability is increased so that it equals the basement membrane water permeability, the reabsorbate remains isotonic and the rate of reabsorption is sensitive to variations of transmural pressure. The major difference between the model with this set of parameters and the model with the reference set is in the path that water takes. With the reference set and a transmural pressure difference of 20 mm Hg, 12% of the reabsorbate enters the channel through the tight junction while the remainder crosses the lateral wall from the cells. With equal permeabilities and a transmural pressure difference of 20 mm Hg, more than 60% of the reabsorbate flow enters across the tight junction. As the tight junction water permeability increases, the model comes to behave as a simple hydraulic shunt. It is difficult to reconcile such large water flows across the tight junction with the results of protein perfusion experiments [16], and so we selected a set of parameters that minimizes but does not eliminate these flows.

We thank R.E. Kalaba for helpful discussions about numerical methods, and Ms. Suzonne Z. Oliver for expert editorial assistance. Preliminary results were reported at the Spring, 1974 Annual Meeting of the American Physiological Society, Atlantic City, N.J. This work was supported in part by NIH Grants AM-15968, HL-15031, and GM-01724.

References

1. Bank, N.W., Erygar, W.E., Aynedjian, H.S. 1971. A microperfusion study of sucrose movement across the rat proximal tubule during renal vein constriction. *J. Clin. Invest.* **50**:294
2. Bellman, R.E., Kalaba, R.E. 1965. Quasilinearization and Nonlinear Boundary-Value Problems. American Elsevier, New York
3. Boulpaep, E.L. 1972. Permeability changes of the proximal tubule of *Necturus* during saline loading. *Amer. J. Physiol.* **222**:517

4. Brenner, B.M., Falchuk, K.H., Keimowitz, R.I., Berliner, R.W. 1969. The relationships between peritubular capillary protein concentration and fluid reabsorption by the proximal tubule. *J. Clin. Invest.* **48**:1519
5. Brenner, B.M., Galla, J.H. 1971. Influence of post-glomerular hematocrit and protein concentration in rat nephron fluid transfer. *Amer. J. Physiol.* **220**:148
6. Brenner, B.M., Troy, J.L. 1971. Post-glomerular vascular protein concentration: Evidence for a causal role in governing fluid reabsorption and glomerulotubular balance by the renal proximal tubule. *J. Clin. Invest.* **50**:336
7. Burg, N.B., Grantham, J.J. 1971. Ion movements in renal tubules. *In:* Membranes and Ion Transport. E.E. Bittar, editor. Vol. 3, p. 49. Wiley-Interscience, London
8. Burg, M.B., Orloff, J. 1968. Control of fluid absorption in the renal proximal tubule. *J. Clin. Invest.* **47**:2016
9. Diamond, J.M. 1974. Tight and leaky junctions of epithelia: A perspective on kisses in the dark. *Fed. Proc.* **33**:2220
10. Diamond, J., Bossert, W.H. 1967. Standing gradient osmotic flow. A mechanism for coupling of water and solute transport in epithelia. *J. Gen. Physiol.* **50**:2061
11. DiBona, D.R., Chen, L.C., Sharp, G.W.G. 1974. A study of intercellular spaces in the rabbit jejunum during acute volume expansion and after treatment with cholera toxin. *J. Clin. Invest.* **53**:1300
12. Frizzell, R.A., Schultz, S.G. 1972. Ionic conductances of extracellular shunt pathway in rabbit ileum. Influence of shunt on transmural sodium transport and electrical potential differences. *J. Gen. Physiol.* **59**:318
13. Frömter, E. 1972. The route of passive ion movement through the epithelium of *Necturus* gallbladder. *J. Membrane Biol.* **8**:259
14. Frömter, E., Diamond, J. 1972. Route of passive ion permeability variation in epithelia. *Nature, New Biol.* **235**:9
15. Gertz, K.H. 1973. Transtubulare Natriumchloridflüsse und Permeabilität für Nichtelektrolyte im proximalen und distalen Convolute der Rattenniere. *Pflug. Archiv.* **276**:336
16. Green, R., Windhager, E.E., Giebisch, G. 1974. Protein oncotic pressure effects on proximal tubular fluid movement in the rat. *Amer. J. Physiol.* **226**:265
17. Humphreys, M.H., Earley, L.E. 1971. The mechanism of decreased intestinal sodium and water reabsorption after acute volume expansion in the rat. *J. Clin. Invest.* **50**:2355
18. Kaye, G.I., Wheeler, H.O., Whitlock, R.T., Lane, N. 1966. Fluid transport in the rabbit gall bladder. A combined physiological and electron microscopic study. *J. Cell. Biol.* **30**:237
19. Kedem, O., Katchalsky, A. 1958. Thermodynamic analysis of the permeability of biological membranes to non-electrolytes. *Biochim. Biophys. Acta* **27**:229
20. Lassiter, W.E., Gottschalk, C.W., Mylle, M. 1961. Micropuncture study of net transtubular movement of water and urea in nondiuretic mammalian kidney. *Amer. J. Physiol.* **200**:1139
21. Lewy, J.E., Windhager, E.E. 1968. Peritubular control of proximal tubular fluid reabsorption in the rat kidney. *Amer. J. Physiol.* **214**:943
22. Lorentz, W.D., Jr., Lassiter, W.E., Gottschalk, C.W. 1971. Renal tubular permeability during increased intra-renal pressure. *J. Clin. Invest.* **51**:484
23. Machen, T.E., Diamond, J.M. 1969. An estimate of the salt concentration in the lateral intercellular spaces of rabbit gall-bladder during maximal fluid transport. *J. Membrane Biol.* **1**:194
24. Martino, J.A., Earley, L.E. 1967. Demonstration of a role of physical factors as determinants of the natriuretic response to volume expansion. *J. Clin. Invest.* **46**:1963
25. Maunsbach, A.B. 1966. The influence of different fixatives and fixation methods on the ultrastructure of rat kidney and rat proximal tubule cells. I. Comparison on different

perfusion fixation methods and of glutaraldehyde formaldehyde and osmium tetroxide fixatives. *J. Ultrastruct. Res.* **15**:242
26. Robinson, R.A., Stokes, R.H. 1959. Electrolyte Solutions. Butterworth, London
27. Seely, J.F. 1973. Effects of peritubular oncotic pressure on rat proximal tubule electrical resistance. *Kidney Internat.* **4**:28
28. Segel, L.A. 1970. Standing gradient flows driven by active solute transport. *J. Theoret. Biol.* **29**:233
29. Spitzer, A., Windhager, E.E. 1970. Effect of peritubular oncotic pressure changes on proximal tubular fluid reabsorption. *Amer. J. Physiol.* **218**:1188
30. Spring, K.R. 1973. Current-induced voltage transients in *Necturus* proximal tubule. *J. Membrane Biol.* **13**:299
31. Tisher, C.C., Kokko, J.T. 1974. Relationship between peritubular oncotic pressure gradients and morphology in isolated proximal tubules. *Kidney Internat.* **6**:146
32. Tormey, J.McD., Diamond, J.M. 1967. The ultrastructural route of fluid transport in rabbit gall bladder. *J. Gen. Physiol.* **50**:2031
33. Ullrich, K.J. 1973. Permeability characteristics of the mammalian nephron. *In:* Handbook of Physiology. Sec. 8, Renal Physiology. J. Orloff and R.W. Berliner, Editors. p. 377. American Physiol. Society, Washington, D.C.
34. Ullrich, K.J., Schmidt-Nielsen, B., Odell, R., Jr., Pehling, G., Gottschalk, C.W., Lassiter, W.E., Mylle, M. 1963. Micropuncture study of composition of proximal and distal tubular fluid in rat kidney. *Amer. J. Physiol.* **204**:527
35. Welling, L.W., Grantham, J.J. 1972. Physical properties of isolated perfused renal tubules and tubular basement membranes. *J. Clin. Invest.* **51**:1063
36. Whittembury, G., Sugino, N., Solomon, A.K. 1961. Ionic permeability and electrical potential differences in *Necturus* kidney cells. *J. Gen. Physiol.* **44**:689
37. Wirz, H. 1956. Der osmotische Druck in den corticalen Tubuli der Rattenniere. *Helv. Physiol. Pharmacol. Acta* **14**:353